Modular model reduction of interconnected systems: A robust performance analysis perspective☆

Lars A.L. Janssen [a],*, Bart Besselink [b], Rob H.B. Fey [a], Nathan van de Wouw [a]

[a] *Dynamics & Control group, Department of Mechanical Engineering, Eindhoven University of Technology, Netherlands*
[b] *Bernoulli Institute for Mathematics, Computer Science and Artificial Intelligence, University of Groningen, Netherlands*

A B S T R A C T

Many complex engineering systems consist of multiple subsystems that are developed by different teams of engineers. To analyse, simulate and control such complex systems, accurate yet computationally efficient models are required. Modular model reduction, in which the subsystem models are reduced individually, is a practical and an efficient method to obtain accurate reduced-order models of such complex systems. However, when subsystems are reduced individually, without taking their interconnections into account, the effect on stability and accuracy of the resulting reduced-order interconnected system is difficult to predict. In this work, a mathematical relation between the accuracy of reduced-order linear-time invariant subsystem models and (stability and accuracy of) resulting reduced-order interconnected linear time-invariant model is introduced. This result can subsequently be used in two ways. Firstly, it can be used to translate accuracy characteristics of the reduced-order subsystem models directly to accuracy properties of the interconnected reduced-order model. Secondly, it can also be used to translate specifications on the interconnected system model accuracy to accuracy requirements on subsystem models that can be used for fit-for-purpose reduction of the subsystem models. These applications of the proposed analysis framework for modular model reduction are demonstrated on an illustrative structural dynamics example.

1. Introduction

Many complex engineering systems, such as those in the automotive and high-tech industry, rely on the integration of multiple interconnected subsystems/modules. These subsystems are increasingly of a multiphysics and/or multidisciplinary nature and their dynamic behaviour is typically developed, modelled, and analysed independently, possibly by distinct teams. For the analysis and design of a single subsystem, detailed high-order models with a high level of complexity are typically used. The dynamics of each subsystem may be modelled and analysed individually in, e.g., the mechanical, electrical or thermal domain, or combinations thereof and control engineers may use these subsystem models to guarantee required dynamic behaviour. Interconnecting such high-order subsystem models to analyse the interconnected system would lead to models of such high complexity that the dynamics analysis of the interconnected system becomes infeasible. Therefore, simplified versions of these subsystem models, i.e., reduced-order models (ROMs), are used instead for analysis of the interconnected system model (Reis & Stykel, 2008). In this paper, we will provide a framework for analysing how the errors introduced by subsystem reduction influence the accuracy of the model of the interconnected system.

The general process of simplifying models, called model order reduction (MOR), is a topic that is studied in several research fields such as structural dynamics (Craig, 2000), systems and control (Gugercin & Antoulas, 2004), thermal systems (Veldman et al., 2018), see Antoulas (2005), Besselink et al. (2013) and Schilders, Van der Vorst, and Rommes (2008) for overviews. Generally, in MOR, the aim is to find a ROM that is reduced significantly in complexity while still providing an accurate description of the dynamic behaviour of the high-order model. For linear systems, this accuracy requirement typically specifies a frequency range of interest. For linear time-invariant (LTI) systems, this is performed commonly using projection-based methods (Antoulas, 2005). These methods rely on the projection of the high-order model onto a subspace with a reduced

number of states. Examples of commonly used projection-based methods used for MOR are the proper orthogonal decomposition method (Kerschen, Golinval, Vakakis, & Bergman, 2005), reduced basis methods (Boyaval et al., 2010), balancing methods (Glover, 1984; Gugercin & Antoulas, 2004; Moore, 1981) and Krylov methods (Grimme, 1997).

Applying these MOR methods on a subsystem level can lead to accurate subsystem models. However, it does not necessarily lead to the best approximation of the behaviour of the *interconnected* system. Therefore, several other approaches have been explored. Although direct reduction of the entire interconnected system as a whole often leads to accurate models, it completely destroys the interconnection structure (Lutowska, 2012). As a solution to this problem, structure-preserving methods are available for interconnected systems (Lutowska, 2012; Sandberg & Murray, 2009; Schilders & Lutowska, 2014; Vandendorpe & van Dooren, 2008). In the structural dynamics field, component mode synthesis (CMS) methods are also structure-preserving (de Klerk, Rixen, & Voormeeren, 2008). However, these methods do not provide a priori error bounds. A complementary approach is model reduction of network systems (Besselink, Sandberg, & Johansson, 2015; Cheng & Scherpen, 2021; Yeung, Goncalves, Sandberg, & Warnick, 2009), where the aim is often to reduce the interconnection structure rather than the subsystem dynamics. Furthermore, for network systems, the interconnected system typically consists of a large number of subsystems of relatively small complexity. Therefore, these methods are not developed for the case of several highly complex interconnected LTI subsystems.

To perform accurate model reduction, knowledge on the entire interconnected system model is needed. However, this is typically not feasible for large-scale models of interconnected systems. In such cases, modular model reduction is the preferred approach (Buhr & Smetana, 2018; Vaz & Davison, 1990), as it provides a significant computational advantage. Additionally, it allows to decompose the overall complexity reduction problem into smaller ones tailored to the nature of the subsystems (Reis & Stykel, 2008). Therefore, a MOR method that is best suitable for reducing a specific subsystem can be chosen for each subsystem individually (Benner, Gugercin, & Willcox, 2015). Furthermore, modular model reduction has the advantage that it preserves the interconnection structure and the physical interpretation of the subsystems. Specifically, in the reduced-order model of the interconnected system, (1) the topology of the system that describes how the subsystems interact, i.e., the interconnection structure, is preserved and, (2) each subsystem model still represents the physical behaviour of that subsystem.

Unfortunately, when a system model is reduced modularly, i.e., individually on a subsystem level, it is challenging to quantify how the stability and accuracy of the reduced-order interconnected system model are affected by a loss of accuracy induced by the reduction of a subsystem model. Although there are some a priori error bounds available in the literature (Ishizaki, Kashima, Imura, & Aihara, 2013; Reis & Stykel, 2008), these are often highly conservative and therefore less suitable for competitive engineering applications. In addition, if there are requirements on accuracy of the interconnected system it is difficult to translate these requirements to subsystem level. Currently, to the best of the authors' knowledge, there is no method that allows to specify accuracy requirements for subsystem models from a global perspective that guarantee a given accuracy for the required overall interconnected system a priori (i.e., before performing the actual reduction).

This paper has the following contributions. The main contribution is a framework for quantitatively relating the input-to-output subsystem model accuracy to input-to-output accuracy of the interconnected system model. This framework is obtained by using a robust performance analysis approach in which model reduction errors are modelled as uncertainties. It allows for a direct implementation of efficient mathematical tools from the theory of robust control (Skogestad & Postlethwaite, 2005; Zhou & Doyle, 1998) such as the structured singular value (Packard & Doyle, 1993). These tools can be used to relate subsystem reduction errors to the reduction error of the interconnected system, thus allowing for analysing and optimizing the accuracy of subsystem reduction. As specific uses of this framework, two additional contributions follow.

First, the modular model reduction is analysed using a bottom-up approach. This approach allows to determine the propagation of errors introduced by subsystem model reduction to the reduced-order interconnected system model. Using this approach, a priori stability guarantees and error bounds on the interconnected system model can be computed using only (a priori) knowledge on reduction errors on a subsystem level. We compare the global a priori error bound to that in Reis and Stykel (2007) and show that it is significantly less conservative for the given example system. In our earlier work (Janssen, Besselink, Fey, Hossein Abbasi, & van de Wouw, 2022), we presented an iterative version this approach using bisection to find a priori error bounds. In this work, these error bounds can be efficiently computed either on a frequency-dependent or global (frequency-independent) level by solving simple linear matrix inequalities (LMIs). Additionally, we show how the error bound can be computed using the actual error of the subsystems, and can therefore also be applied to MOR methods for which a priori error bounds are not available, such as Krylov or CMS methods.

Second, a top-down approach is given. In this approach, accuracy specifications on a subsystem level are determined based on requirements on the interconnected system model accuracy. Typically, we are interested in obtaining a (reduced) model of the interconnected system that meets some specific accuracy requirements. With this approach, by solving simple LMIs, we can translate these accuracy requirements to the subsystem level. Therefore, model reduction can be applied on a subsystem level. In particular, this allows for the use of different MOR methods for different subsystems, as long as error bound requirements are met.

The paper is organized as follows. Section 2 gives the problem statement including the modelling framework. In Section 3, a robust performance perspective on modular model reduction is developed, i.e., it is explained how to relate subsystem model reduction errors to the reduced-order interconnected system model error and vice versa. Specific applications of these relations, i.e., the bottom-up and top-down approaches, are given in Section 4 which are demonstrated on an illustrative structural dynamics example system in Section 5. The conclusions and recommendations for future work are given in Section 6.

Notation. The set of real numbers is denoted by $\mathbb{R}$. The set of complex numbers is denoted by $\mathbb{C}$. Given a vector $x \in \mathbb{C}^n$, its Euclidean norm is given as $\|x\|$. Given a transfer function (matrix) $G(s)$, where s is the Laplace variable, $\|G\|_\infty$ denotes its $\mathcal{H}_\infty$-norm. The real rational subspace of $\mathcal{H}_\infty$ is denoted by $\mathcal{RH}_\infty$, which consists of all proper and real rational stable transfer matrices. Given a complex matrix A, A^H denotes its conjugate transpose, $\bar{\sigma}(A)$ denotes its largest singular value, $\rho(A)$ denotes its spectral radius and $A = \text{diag}(A_1, A_2)$ denotes a block-diagonal matrix with submatrices A_1 and A_2. The identity matrix of size n is denoted by I_n.

2. Problem statement

In this work, we consider a set of arbitrarily interconnected LTI subsystems. These subsystems interact by linking for each
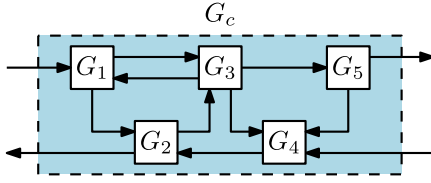
Fig. 1. Block diagram representation an arbitrarily interconnected system consisting of several subsystems.
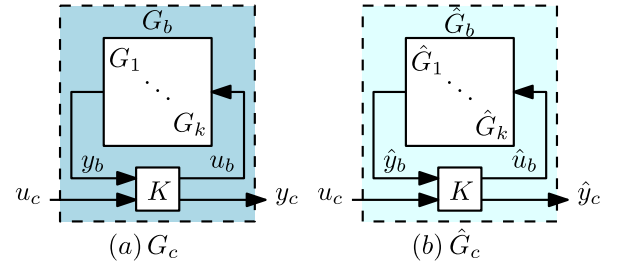

Fig. 2. Block diagram representation of (a) high-order interconnected system $G_c(s)$ and (b) reduced-order interconnected system $\hat{G}_c(s)$. K represents a static interconnection block.

subsystem, (a part of) subsystem outputs, to (a part of) inputs of the other subsystems. Additionally, some subsystems will have one or multiple external input(s) and/or output(s). An example of such a system is given in Fig. 1. This class of systems contains a wide variety of interconnected systems for which model reduction is essential to enable design, analysis and control of the system dynamics.

2.1. Modular model framework

Consider k high-order subsystems $j \in \{1, \ldots, k\}$ with (proper real rational) transfer functions $G_j(s)$, inputs u_j and outputs y_j of dimensions m_j and p_j, respectively, and McMillan degree n_j. We collect the subsystem transfer functions in the block-diagonal transfer function

$$G_b(s) := \text{diag}(G_1(s), \ldots, G_k(s)), \tag{2.1}$$

for which the total number of inputs and outputs are then given by $m_b := \sum_{j=1}^{k} m_j$ and $p_b := \sum_{j=1}^{k} p_j$, respectively. We define inputs $u_b^\top := [u_1^\top, \ldots, u_k^\top]$ and outputs $y_b^\top := [y_1^\top, \ldots, y_k^\top]$.

The subsystems are interconnected according to

$$\begin{bmatrix} u_b \\ y_c \end{bmatrix} = K \begin{bmatrix} y_b \\ u_c \end{bmatrix}, \qquad K = \begin{bmatrix} K_{11} & K_{12} \\ K_{21} & K_{22} \end{bmatrix} \tag{2.2}$$

where u_c and y_c denote external inputs and outputs, respectively, see Fig. 2(a). The number of external inputs and outputs are given by m_c and p_c, respectively. Then, the transfer function from u_c to y_c is given by the upper linear fractional transformation (LFT) of $G_b(s)$ and K, which yields

$$G_c(s) := K_{21} G_b(s)(I - K_{11} G_b(s))^{-1} K_{12} + K_{22}. \tag{2.3}$$

Throughout this paper, we make the following assumption.

Assumption 2.1. The system (2.3) is

(1) well-posed, i.e., $I - K_{11} G_b(s)$ has a proper real rational inverse;
(2) is internally stable, i.e., $(I - K_{11} G_b(s))^{-1} \in \mathcal{RH}_\infty$ and $G_c(s) \in \mathcal{RH}_\infty$.

Note that a feedback system is defined to be well-posed if *all* closed-loop transfer functions are well-defined and proper, and internally stable if *all* closed-loop transfer functions are stable. Because K is a *static* interconnection matrix, the specified transfer functions in Assumption 2.1 are necessary and sufficient for their respective properties on $G_c(s)$. For a potential extension to a *dynamic* interconnection structure $K(s)$, additional assumptions are required that guarantee the well-posedness and internal stability of (2.3). For more details on well-posedness and internal stability, see Zhou and Doyle (1998, Definitions 5.1 and 5.2). Note that for many systems within this modelling framework, external inputs and outputs are directly connected to a subsystem input and output, respectively. In those instances, u_c will contain identical elements in u_b. The same holds for output signals y_c and y_b.

2.2. Modular model order reduction

In model order reduction, we aim to find a ROM of a system with (significantly) fewer internal states than the number of states of the high-order model. In this paper, we compute the ROM of the system modularly, i.e., we reduce each subsystem independently. Therefore, we need to consider reduced-order subsystems $j \in \{1, \ldots, k\}$ and their (real rational proper) transfer functions $\hat{G}_j(s)$, each with inputs $\hat{u}_j$ and outputs $\hat{y}_j$ with dimensions m_j and p_j, respectively, and McMillan degree r_j. Let the reduced-order block-diagonal transfer function be given as

$$\hat{G}_b(s) := \text{diag}(\hat{G}_1(s), \ldots, \hat{G}_k(s)). \tag{2.4}$$

Then, we define inputs $\hat{u}_b^\top := [\hat{u}_1^\top, \ldots, \hat{u}_k^\top]$ and outputs $\hat{y}_b^\top := [\hat{y}_1^\top, \ldots, \hat{y}_k^\top]$ with dimensions m_b and p_b, respectively. Since we only reduce the subsystem models, the interconnection structure remains preserved. Therefore, the reduced-order interconnected system transfer function is, similar to (2.3), given by

$$\hat{G}_c(s) := K_{21} \hat{G}_b(s)(I - K_{11} \hat{G}_b(s))^{-1} K_{12} + K_{22}. \tag{2.5}$$

Here, the reduced-order interconnected system has external inputs u_c and external outputs $\hat{y}_c$. The reduced-order interconnected system is illustrated in Fig. 2(b). Note that we do not make any assumptions on well-posedness and stability of (2.5). In fact, we would like to find conditions on the model reduction procedure that guarantees these properties given the high-order model $G_c(s)$ satisfying Assumption 2.1.

In this paper, the aim is to compute a ROM that can accurately describe the external input-to-output behaviour of the interconnected system. In the described modelling framework, this means that given the same external input u_c, the difference between the external output signal of the high-order and the reduced-order system $e_c := \hat{y}_c - y_c$, is required to be small. Therefore, the accuracy of the reduced-order interconnected system can be described by the interconnected system error dynamics, which is defined as

$$E_c(s) := \hat{G}_c(s) - G_c(s). \tag{2.6}$$

Given (2.3), (2.5) and (2.6), E_c can be written as

$$\begin{aligned} E_c(s) = \quad & K_{21} \hat{G}_b(s)(I - K_{11} \hat{G}_b(s))^{-1} K_{12} \\ & - K_{21} G_b(s)(I - K_{11} G_b(s))^{-1} K_{12}. \end{aligned} \tag{2.7}$$

However, with a modular approach, subsystems are reduced independently, which therefore means that knowledge on the accuracy of the reduced models is generally only available on a *subsystem level*. The accuracy of the reduced-order subsystems can be described by the subsystem error dynamics, which is defined as

$$E_j(s) := \hat{G}_j(s) - G_j(s). \tag{2.8}$$

The associated output error is denoted as $e_j = \hat{y}_j - y_j$. We assume that the reduction is such that $E_j(s) \in \mathcal{RH}_\infty$.

Remark 2.2. For some model reduction methods, bounds on the error dynamics are available a priori. For example, model reduction using traditional balanced truncation (Enns, 1984; Moore, 1981) can be applied to systems satisfying $G_j(s) \in \mathcal{RH}_\infty$. It guarantees preservation of stability, i.e., $\hat{G}_j(s) \in \mathcal{RH}_\infty$, and therefore $E_j(s) \in \mathcal{RH}_\infty$. The a priori error bound on the reduced-order subsystem j is then given by

$$\|E_j\|_\infty \leq \sum_{i=r+1}^{n_j} \sigma_{j,i}. \tag{2.9}$$

Here, $\sigma_{j,i}, i = 1, \ldots, n_j$ are the Hankel singular values (Glover, 1984).

Computation of the reduction error of the interconnected system E_c on the basis of knowledge of E_j can be computationally expensive or even infeasible for complex interconnected high-order models. Moreover, this computation is only possible when the *exact* subsystem reduction errors E_j are known for all subsystems.

In addition, usually, requirements are posed to model accuracy and model complexity on the *level of the interconnected system*. With modular model reduction however, the subsystem models are reduced on *subsystem level*. Therefore, the need arises for establishing a relation between subsystem error dynamics E_j and the interconnected system error dynamics E_c without exact a priori knowledge of the specific error dynamics E_j for all subsystems. In the next section, we will show how this relation can be formulated using a robust performance analysis perspective. Specifically, we will show how this relation gives the ability to pursue

(1) *a bottom-up approach*: evaluate the propagation of subsystem reduction errors E_j to the resulting stability and accuracy of the reduced interconnected system E_c, and

(2) *a top-down approach*: determine requirements on the subsystem reduction error dynamics E_j to meet requirements on stability and specified maximal error E_c of the reduced interconnected system.

3. A robust performance perspective on modular model reduction

In this section, we show how reformulation of the modular model reduction framework into a robust performance analysis problem setting can lead to a directly computable relation between E_j and E_c. To this end, we recall that $E_j(s) \in \mathcal{RH}_\infty$. As a result, we can define weighting transfer functions $V_j(s) \in \mathcal{RH}_\infty$ and $W_j(s) \in \mathcal{RH}_\infty$ such that $E_j(s)$ can be written as

$$E_j(s) = W_j(s)\Delta_j(s)V_j(s), \tag{3.1}$$

for some $\Delta_j(s) \in \mathcal{RH}_\infty$ satisfying $\|\Delta_j\|_\infty \leq 1$. Such formulation is standard in robust control theory, see e.g. Skogestad and Postlethwaite (2005, Section 8.2.3). Then, (2.8) can be rewritten as

$$\hat{G}_j(s) = G_j(s) + W_j(s)\Delta_j(s)V_j(s). \tag{3.2}$$

This representation is shown in Fig. 3. Similar to before, we collect the matrices Δ_j and the weighting matrices as

$$\Delta_b(s) := \text{diag}(\Delta_1(s), \ldots, \Delta_k(s)),$$
$$V_b(s) := \text{diag}(V_1(s), \ldots, V_k(s)), \text{ and}$$
$$W_b(s) := \text{diag}(W_1(s), \ldots, W_k(s)).$$

such that we have $E_b(s) = \hat{G}_b(s) - G_b(s) = W_b(s)\Delta_b(s)V_b(s)$.

By replacing $\hat{G}_b(s)$ by $G_b(s) + W_b(s)\Delta_b(s)V_b(s)$ in Fig. 2(b) and comparing it with the high-order system $G_b(s)$ in Fig. 2(a), we obtain the block diagram in Fig. 4. This allows us to rewrite the
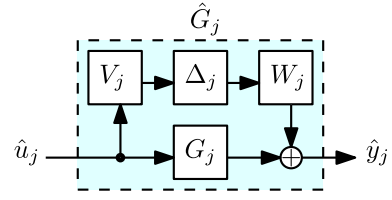

Fig. 3. Block diagram representation of $\hat{G}_j(s) = G_j(s) + E_j(s)$ where $E_j(s)$ is given as a function of $V_j(s)$, $W_j(s)$ and $\Delta_j(s)$.

interconnected system error dynamics $E_c(s)$ as in (2.7) as an upper LFT of block-diagonal weighting transfer functions $W_b(s)$, $V_b(s)$, the block-diagonal transfer function $\Delta_b(s)$, and the nominal transfer function $N(s)$ given by

$$N(s) = \begin{bmatrix} N_{11}(s) & N_{12}(s) \\ N_{21}(s) & O \end{bmatrix}, \tag{3.3}$$

where

$$N_{11}(s) = K_{11}(I - G_b(s)K_{11})^{-1},$$
$$N_{12}(s) = (I - K_{11}G_b(s))^{-1}K_{12}, \tag{3.4}$$
$$N_{21}(s) = K_{21}(I - G_b(s)K_{11})^{-1}.$$

Note that we have $N(s) \in \mathcal{RH}_\infty$ as a result of Assumption 2.1. Fig. 4 shows the inputs and outputs of the nominal system $N(s)$. The transfer function of the interconnected system error dynamics E_c is then given by

$$E_c(s) = N_{21}W_b\Delta_bV_b(I - N_{11}W_b\Delta_bV_b)^{-1}N_{12}. \tag{3.5}$$

As is standard within robust control theory (Zhou & Doyle, 1998), with (3.5), in $E_c(s)$, we have now "pulled out" the errors introduced by the reduction of subsystems $G_j(s)$ from the nominal system $N(s)$ and shifted them into $V_b(s)$, $W_b(s)$ and $\Delta_b(s)$. The remaining system $N(s)$ consists only of high-order models $G_b(s)$ and their interconnection structure K, see (3.3), and is thus known before reduction is applied to any of the subsystems.

In robust control theory (Packard & Doyle, 1993; Skogestad & Postlethwaite, 2005; Zhou & Doyle, 1998), by definition, a system satisfies a robust performance criterion if for all perturbed plants within the set of uncertain system models it satisfies the given performance specifications. In doing so, it gives a worst-case relation between local uncertainties in the system to the global performance of this system. In this paper, by reformulation of the problem, robust performance analysis methods can be exploited to study the relation between $E_j(s)$ and $E_c(s)$.

Up to now, we have extracted the errors introduced by reduction of the subsystems through the terms $\Delta_b(s)$, $W_b(s)$ and $V_b(s)$. As we aim to relate these subsystem reduction errors to the global reduction error $E_c(s)$, it will turn out to be useful to introduce a feedback between e_c and u_c in Fig. 4, leading to Fig. 5, as is typical in robust performance analysis (Zhou & Doyle, 1998, Figure 10.5). In this setup, the relation between local and global reduction errors can be regarded as a robust performance problem. To make this explicit, define $\Delta_c(s)$ and weighting transfer functions $V_c(s)$ and $W_c(s)$ which represent a performance specification on the interconnected system error dynamics $E_c(s)$. By closing this loop as in Fig. 5, the robust performance problem becomes equivalent to a robust stability problem with augmented functions $\Delta_c(s)$, $V_c(s)$ and $W_c(s)$ (Zhou & Doyle, 1998, Theorem 10.8). Furthermore, we define transfer functions

$$\Delta(s) := \text{diag}(\Delta_b(s), \Delta_c(s)),$$
$$V(s) := \text{diag}(V_b(s), V_c(s)), \text{ and} \tag{3.6}$$
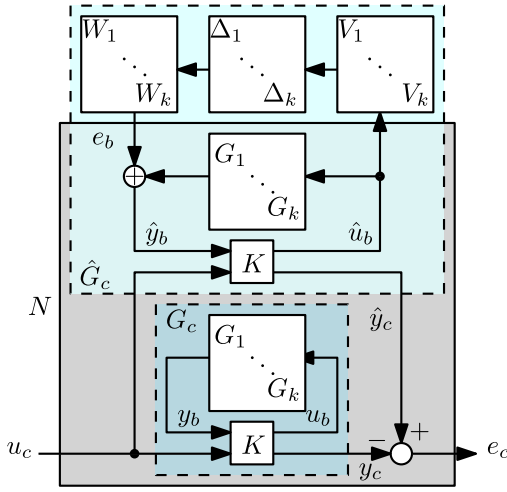$$W(s) := \text{diag}(W_b(s), W_c(s)),$$

Fig. 4. Block diagram representation of the error dynamics of the interconnected system, $E_c(s) = \hat{G}_c(s) - G_c(s)$, as a function of $V_b(s)$, $W_b(s)$, $\Delta(s)$ and the nominal system $N(s)$.
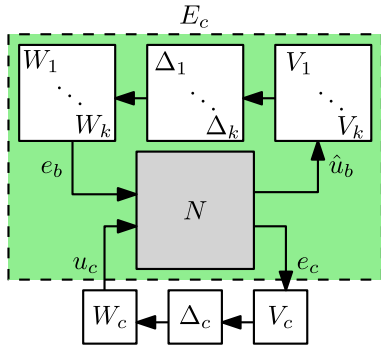

Fig. 5. Block diagram representation of the error dynamics of the interconnected system, $E_c(s) = \hat{G}_c(s) - G_c(s)$, including the nominal system $N(s)$, augmented uncertainty $\Delta_c(s)$ and weighting transfer functions $V_c(s)$, $W_c(s)$ for robust performance analysis.

and let $V, V^{-1}, W, W^{-1} \in \mathcal{RH}_\infty$. Note that the stability property of these transfer functions can always be ensured by appropriate selection of these (weighting) functions $V(s)$ and $W(s)$. In Section 4, we show that, for specific weighting functions, this allows for the establishment of bottom-up and top-down relations between the errors E_c and E_j.

If the error dynamics $E_b(s) \in \mathcal{RH}_\infty$ and $E_c(s) \in \mathcal{RH}_\infty$ are known exactly, by definition, a solution to $\Delta_b(s)$, $V_b(s)$ and $W_b(s)$ can be found. However, to have the ability to solve both the bottom-up and top-down problems, as described at the end of Section 2, we will at this point no longer assume that $E_b(s)$ and $E_c(s)$ are known (a priori). Instead of working with given exact error dynamics $E_b(s)$ and $E_c(s)$, we consider a larger (uncertainty) set of error dynamics that contains $E_b(s)$ and $E_c(s)$. To define this, consider the set Δ as the set of complex matrices structured accordingly as

$$\Delta := \Big\{ \mathrm{diag}\big(\Delta_1, \ldots, \Delta_k, \Delta_c\big) \ \Big| \tag{3.7}$$
$$\Delta_j \in \mathbb{C}^{p_j \times m_j}, j \in \{1, \ldots, k\}, \Delta_c \in \mathbb{C}^{m_c \times p_c} \Big\}.$$

Given Δ, the MOR problem is reformulated as a robust performance problem where the error dynamics $E_b(s)$ and the performance specification on $E_c(s)$ are represented as an uncertain system bounded by Δ and the weighting functions $W(s)$ and $V(s)$.

Therefore, computational tools from the field of robust control, specifically, the structured singular value μ, can be used.

Definition 3.1 (*Packard and Doyle (1993, Definition 3.1)*)**.** Given matrix $M \in \mathbb{C}^{(m_b + p_c) \times (p_b + m_c)}$, the structured singular value is

$$\mu_\Delta(M) := \frac{1}{\min\{\bar{\sigma}(\Delta) \mid \det(I - M\Delta) = 0, \Delta \in \Delta\}}. \tag{3.8}$$

Here, $\mu_\Delta(M)$ is the smallest $\Delta \in \Delta$, in terms of $\bar{\sigma}(\Delta)$, that makes the matrix $I - M\Delta$ singular. Using ideas from robust performance analysis, we pose the following theorem.

Theorem 3.2. *Consider the system* (2.3) *satisfying* Assumption 2.1, *weighting functions* (3.6), *and the error dynamics* (3.5) *in* Fig. 4. *The following statements are equivalent:*

(1) For any $E_j(s) \in \mathcal{RH}_\infty$ satisfying

$$\|W_j^{-1} E_j V_j^{-1}\|_\infty \le 1, \tag{3.9}$$

$j \in \{1, \ldots, k\}$, we have that the error dynamics (3.5) *are well-posed, internally stable, and satisfy*

$$\|V_c E_c W_c\|_\infty < 1. \tag{3.10}$$

(2) With Δ as in (3.7),

$$\sup_{\omega \in \mathbb{R}} \mu_\Delta \big(V(i\omega) N(i\omega) W(i\omega)\big) < 1. \tag{3.11}$$

Proof. With the following remarks, we show that the theorem becomes equivalent to the robust performance criterion, as given in Skogestad and Postlethwaite (2005, Theorem 8.7) and Zhou and Doyle (1998, Theorem 10.8).

(1) We have that $N \in \mathcal{RH}_\infty$ as a result of Assumption 2.1 and weighting functions (3.6) we have $VNW \in \mathcal{RH}_\infty$.
(2) Let

$$\Delta_\mathbf{b} := \Big\{ \mathrm{diag}\big(\Delta_1, \ldots, \Delta_k\big) \ \Big|$$
$$\Delta_j \in \mathbb{C}^{p_j \times m_j}, j \in \{1, \ldots, k\} \Big\}. \tag{3.12}$$

Then, due to the block-diagonal structure of E_b and the weighting filters V_b and W_b, we have,

$$W_b^{-1} E_b V_b^{-1}(i\omega) \in$$
$$\Big\{ \Delta_b \in \mathcal{RH}_\infty \Big| \Delta_b(s) \in \Delta_\mathbf{b} \ \forall \ s \in \mathbb{C} \Big\}. \tag{3.13}$$

(3) The system $V_c E_c W_c$ is the upper LFT of weighted nominal system VNW and uncertainty Δ_b as in (3.13).
(4) With Δ as in (3.7), we have the augmented block structure to test the robust performance of the system in Fig. 4. Note that Fig. 5 is equivalent to Zhou and Doyle (1998, Figure 10.5). □

Theorem 3.2 is a reformulation of the robust performance criterion using μ-analysis. Using this reformulation, it provides a worst-case relation between the $\mathcal{H}_\infty$-norm of E_j for all $j \in \{1, \ldots, k\}$ and E_c. Note that to verify the satisfaction of (3.11), computationally efficient algorithms have been developed to compute the peak structured singular value, using the algorithms developed for $\mathcal{H}_\infty$-norm computation (Boyd, Balakrishnan, & Kabamba, 1989; Bruinsma & Steinbuch, 1990). See Zhou and Doyle (1998, Section 10.3) for more information.

With weighting transfer functions V and W, it can be computed how certain error dynamics (as described in V_j and W_j) in subsystems E_j affect the interconnected system error dynamics E_c in the worst case. Additionally, Theorem 3.2 implies that the

reduced-order interconnected system $\hat{G}_c$ is stable if the high-order interconnected system G_c is stable and (3.11) is satisfied, as is shown in the following corollary.

Corollary 3.3. *Let the conditions in Theorem 3.2 hold. Then, if (3.11) is satisfied, the reduced-order interconnected system satisfies $\hat{G}_c \in \mathcal{RH}_\infty$.*

Proof. We have that under the conditions in Theorem 3.2,

(1) $G_c \in \mathcal{RH}_\infty$, and
(2) $E_c \in \mathcal{RH}_\infty$ if (3.11) is satisfied.

Therefore, we have that the parallel connection $\hat{G}_c = G_c + E_c \in \mathcal{RH}_\infty$. □

Furthermore, rephrasing Theorem 3.2 such that it provides similar bounds on a frequency-dependent level can now be formalized in the following theorem.

Theorem 3.4. *Consider the system (2.3) satisfying Assumption 2.1, weighting functions (3.6), and the error dynamics (3.5) in Fig. 4. Let $\omega \in \mathbb{R}$. Then, the following statements are equivalent:*

(1) For any $E_j(i\omega)$ satisfying

$$\bar{\sigma}\left(W_j^{-1}(i\omega)E_j(i\omega)V_j^{-1}(i\omega)\right) \leq 1, \tag{3.14}$$

$j \in \{1, \ldots, k\}$, we have that the error dynamics (3.5) satisfy

$$\bar{\sigma}\left(V_c(i\omega)E_c(i\omega)W_c(i\omega)\right) < 1 \tag{3.15}$$

(2) With Δ as in (3.7),

$$\mu_\Delta\left(V(i\omega)N(i\omega)W(i\omega)\right) < 1. \tag{3.16}$$

Proof. This follows similarly to the proof of Theorem 3.2. However, here, Zhou and Doyle (1998, Theorem 10.8) is applied for each frequency individually, such as for example in Zhou and Doyle (1998, Example 10.4). □

Note that for Theorem 3.4, we lose the guarantees on well-posedness and internal stability as μ_Δ is only computed for each frequency individually. To guarantee well-posedness and internal stability of the system, satisfying (3.11) of Theorem 3.2 is sufficient.

Both Theorems 3.2 and 3.4 characterize a flexible relation between E_j and E_c. However, computing μ_Δ has been established to be an NP-hard problem (Young, Newlin, & Doyle, 1991). Fortunately, computing an upper bound on μ_Δ is possible and sufficient to satisfy the condition on μ_Δ in Theorems 3.2 and 3.4 (Skogestad & Postlethwaite, 2005). To this end, consider the set of scaling matrices given as

$$\mathbf{D} := \left\{ (D_\ell, D_r) \,\middle|\, D_\ell = \mathrm{diag}\left(d_1 I_{p_1}, \ldots, d_k I_{p_k}, d_c I_{m_c}\right), \right.$$
$$D_r = \mathrm{diag}\left(d_1 I_{m_1}, \ldots, d_k I_{m_k}, d_c I_{p_c}\right),$$
$$\left. d_1, \ldots, d_k, d_c \in \mathbb{R}_{>0} \right\}. \tag{3.17}$$

Here, we recall that m_j and p_j are the number of inputs and outputs of subsystem j, respectively. We now formulate the following theorem, which is a minor extension of Packard and Doyle (1993, Theorem 3.9).

Theorem 3.5. *Let $M \in \mathbb{C}^{(m_b+p_c)\times(p_b+m_c)}$. If there exists a $(D_\ell, D_r) \in \mathbf{D}$ such that*

$$MD_r M^H \prec D_\ell, \tag{3.18}$$

then, given Δ as in (3.7), $\mu_\Delta(M) < 1$.

Proof. For any $(D_\ell, D_r) \in \mathbf{D}$, we have, as given in Zhou and Doyle (1998, Section 10.2.2), the upper bound

$$\mu_\Delta(M) \leq \bar{\sigma}(D_\ell^{-\frac{1}{2}} M D_r^{\frac{1}{2}}). \tag{3.19}$$

Therefore, to verify $\mu_\Delta(M) < 1$ it is sufficient to find some $(D_\ell, D_r) \in \mathbf{D}$ for which $\bar{\sigma}(D_\ell^{-\frac{1}{2}} M D_r^{\frac{1}{2}}) < 1$. Note that this is equivalent to $(D_\ell^{-\frac{1}{2}} M D_r^{\frac{1}{2}})(D_\ell^{-\frac{1}{2}} M D_r^{\frac{1}{2}})^H \prec I$ and therefore to the matrix inequality

$$D_\ell^{-\frac{1}{2}} M D_r M^H D_\ell^{-\frac{1}{2}} \prec I. \tag{3.20}$$

Finally, we can left- and right-multiply both sides of (3.20) with $D_\ell^{\frac{1}{2}}$ to find (3.18) in the statement of the theorem. □

Note that $V(i\omega)N(i\omega)W(i\omega) \in \mathbb{C}^{(m_b+p_c)\times(p_b+m_c)}$ and let $\omega \in \mathbb{R}$. It follows directly from Theorem 3.5 that if there exists a $(D_\ell, D_r) \in \mathbf{D}$ for which

$$V(i\omega)N(i\omega)W(i\omega)D_r W^H(i\omega)N^H(i\omega)V^H(i\omega) \prec D_\ell, \tag{3.21}$$

we have $\mu_\Delta(V(i\omega)N(i\omega)W(i\omega)) < 1$. For any fixed V, W and N, verifying (3.21) can be done using standard LMI solvers. Solving an LMI can be a computationally expensive task. However, the dimensions of the LMI in (3.21) are $(m_b + p_c) \times (p_b + m_c)$, i.e., based on the number of internal and external inputs in the system. Therefore, the computational cost of solving (3.21) scales with the size of the interconnection structure, and, crucially, not with the number of states in the system. For systems with very complex interconnections, methods that reduce the complexity of the interconnection, such as interface reduction (Krattiger et al., 2019), may be considered.

Remark 3.6. Note that condition (3.11) in Theorem 3.2 requires taking a supremum over ω. Several approaches are available to avoid the computational cost of computing $\mu_\Delta(V(i\omega)N(i\omega)W(i\omega))$ or its upper bound for all $\omega \in \mathbb{R}$. Some of these methods are discussed in detail in Packard and Doyle (1993, Section 10).

Bringing specific structure to V and W, the matrix inequality in (3.21) can be solved such that relations between E_j for all $j \in \{1, \ldots, k\}$ and E_c can be directly computed. These relations provide for instance an error bound on the reduced-order interconnected system model given error bounds of the reduced-order subsystem models (bottom-up approach), and may be used to improve the reduced-order interconnected system model accuracy by reducing subsystem models to satisfy accuracy requirements on the reduced-order interconnected system model (top-down approach). In the next section, guidelines are given on how V and W can be designed specifically for these purposes in the scope of modular model reduction.

4. Error analysis for modular model reduction

With the relations given in Theorems 3.2 and 3.4, the weighting transfer functions V and W can be used to compute how subsystem error dynamics E_j and the interconnected system error dynamics E_c are related to each other, by checking if (3.11) and (3.16) hold for Theorems 3.2 and 3.4, respectively. In this section, we show several approaches to analyse how subsystem error bounds relate to the interconnected system error bounds. These approaches rely on obtaining these relations by imposing a specific structure on the weighting transfer functions V and W. It is shown how relations between bounds on E_j and E_c can be found on a global and frequency-dependent level. These relations will be used for the bottom-up and the top-down approaches, as indicated at the end of Section 2.

4.1. Bottom-up approach: Error bounds on E_c given error bounds on E_j

In this section, we show how to find global and frequency-dependent a priori bounds on the interconnected error dynamics E_c given bounds on the error dynamics E_j for all $j \in \{1, \ldots, k\}$ introduced by reduction of subsystems, and based on Theorems 3.2, 3.4 and 3.5. In the bottom-up approach, we adopt the assumption that for each subsystem $j \in \{1, \ldots, k\}$ we have either an a priori global (frequency-independent) error bound or a frequency-dependent error bound. We then aim to find in the former case a global error bound and in the latter case a frequency-dependent error bound on the interconnected system by proper choices of weighting functions.

The following theorem can be used to compute a global bound $\bar{\varepsilon}_c$ on the interconnected system reduction error, i.e., we have that $\|E_c\|_\infty \leq \bar{\varepsilon}_c$ given $\|E_j\|_\infty \leq \bar{\varepsilon}_j$ for all $j \in \{1, \ldots, k\}$.

Theorem 4.1. Let $E_j \in \mathcal{RH}_\infty$ and let $\bar{\varepsilon}_j$ be such that $\|E_j\|_\infty \leq \bar{\varepsilon}_j$ for all $j \in \{1, \ldots, k\}$. Consider the optimization problem

$$
\begin{aligned}
& given && \bar{\varepsilon}_j \; \forall j \in \{1, \ldots, k\} \\
& \underset{D_\ell, D_r, W^G}{minimize} && \bar{\varepsilon}_c \\
& subject\ to && N(i\omega)W^G D_r W^G N^H(i\omega) \prec D_\ell \; \forall \, \omega, \\
& && (D_\ell, D_r) \in \mathbf{D}
\end{aligned}
\tag{4.1}
$$

with $W^G := diag(\bar{\varepsilon}_1 I_{m_1}, \ldots, \bar{\varepsilon}_k I_{m_k}, \bar{\varepsilon}_c^{-1} I_{p_c})$ and $\mathbf{D}$ as in (3.17). If $\bar{\varepsilon}_c^\star$ is a feasible solution to (4.1), then

  (1) E_c is well-posed,
  (2) E_c is internally stable, and
  (3) $\|E_c\|_\infty < \bar{\varepsilon}_c^\star$.

Proof. The proof follows from Theorems 3.2 and 3.5. By substitution of $V = I_{p_b+m_c}$ and $W = W^G$ for the weighting transfer functions in Theorem 3.2, we have that the feedback system as shown in Fig. 5 is well-posed, internally stable, and

$$
\begin{aligned}
& \|E_c\|_\infty < \bar{\varepsilon}_c \text{ for all} \\
& \|E_j\|_\infty \leq \bar{\varepsilon}_j, \; \forall j \in \{1, \ldots, k\},
\end{aligned}
\tag{4.2}
$$

if and only if $\sup_{\omega \in \mathbb{R}} \mu_\Delta(N(i\omega)W^G) < 1$. Following from Theorem 3.5, this holds if, for all $\omega \in \mathbb{R}$, there exists a $(D_\ell, D_r) \in \mathbf{D}$ such that $N(i\omega)W^G D_r W^G N^H(i\omega) \prec D_\ell$, which is guaranteed by the constraint in (4.1). $\square$

Theorem 4.1 provides a method to guarantee the stability of the reduced-order interconnected system and compute a global upper bound to the $\mathcal{H}_\infty$-norm of the error dynamics of the interconnected system $\|E_c\|_\infty \leq \bar{\varepsilon}_c^\star$ introduced by reduction errors (globally) bounded by $\|E_j\|_\infty \leq \bar{\varepsilon}_j$ for all $j \in \{1, \ldots, k\}$.

Remark 4.2. If we multiply the scaling matrices $(D_\ell, D_r) \in \mathbf{D}$ by any scalar $\alpha > 0$, the resulting scaled largest singular value for any matrix M is given by

$$
\bar{\sigma}\left(\frac{1}{\sqrt{\alpha}} D_\ell^{-\frac{1}{2}} M \sqrt{\alpha} D_r^{\frac{1}{2}}\right) = \bar{\sigma}\left(D_\ell^{-\frac{1}{2}} M D_r^{\frac{1}{2}}\right).
\tag{4.3}
$$

Therefore, if we set any single d_j or d_c in (3.17) to a fixed value greater than zero, which can be achieved by choosing an appropriate value for α, the upper bound to the structured-singular value remains unchanged.

To solve (4.1), we select $d_c = 1$ as this does not change the upper bound on μ_Δ (see Remark 4.2). In this case, we have

$$
W^G D_r W^G = diag(d_1 \bar{\varepsilon}_1^2 I_{m_1}, \ldots, d_k \bar{\varepsilon}_k^2 I_{m_2}, \frac{1}{\bar{\varepsilon}_c^2} I_{p_c}).
\tag{4.4}
$$

As the decision variable of the optimization problem (4.1) appears linearly in (4.4) after setting $\gamma := \bar{\varepsilon}_c^{-2}$, the constraint in (4.1) is a *linear* matrix inequality, i.e., the decision variables $d_1, \ldots, d_k$ and γ appear linearly in (4.1). The solution to problem (4.1) can then be computed directly using standard semidefinite programming (SDP) solvers by maximizing over γ. Note that if no feasible solution can be found, neither well-posedness, stability, nor an error bound can be guaranteed.

For a frequency-dependent relation between E_j and E_c, we introduce the following theorem that can be applied to any (discrete set of frequencies) $\omega \in \mathbb{R}$.

Theorem 4.3. Let ω in $\mathbb{R}$. Let $\varepsilon_j(\omega)$ be such that $\bar{\sigma}(E_j(i\omega)) \leq \varepsilon_j(\omega)$ for all $j \in \{1, \ldots, k\}$. Consider the optimization problem

$$
\begin{aligned}
& given && \varepsilon_j(\omega) \; \forall j \in \{1, \ldots, k\} \\
& \underset{D_\ell, D_r, W^F(\omega)}{minimize} && \varepsilon_c(\omega) \\
& subject\ to && N(i\omega)W^F(\omega) D_r W^F(\omega) N^H(i\omega) \prec D_\ell, \\
& && (D_\ell, D_r) \in \mathbf{D}
\end{aligned}
\tag{4.5}
$$

with $W^F(\omega) := diag(\varepsilon_1(\omega) I_{m_1}, \ldots, \varepsilon_k(\omega) I_{m_k}, \varepsilon_c^{-1}(\omega) I_{p_c})$ and $\mathbf{D}$ as in (3.17). If $\varepsilon_c^\star(\omega)$ is a feasible solution to (4.5), then $\bar{\sigma}(E_c(i\omega)) < \varepsilon_c(\omega)$.

Proof. The proof follows from Theorems 3.4 and 3.5. By substitution of $V = I_{p_b+m_c}$ and $W(i\omega) = W^F(\omega)$ in Theorem 3.4, we obtain

$$
\begin{aligned}
& \bar{\sigma}\left(E_c(i\omega)\right) < \varepsilon_c(\omega) \text{ for all} \\
& \bar{\sigma}\left(E_j(i\omega)\right) \leq \varepsilon_j(\omega) \; \forall j \in \{1, \ldots, k\},
\end{aligned}
\tag{4.6}
$$

if and only if $\mu_\Delta\left(N(i\omega)W^F(\omega)\right) < 1$. Following from Theorem 3.5, this holds if there exists a $(D_\ell, D_r) \in \mathbf{D}$ such that $N(i\omega)W^F(\omega) D_r W^F(\omega) N^H(i\omega) \prec D_\ell$. This matrix inequality is guaranteed by the constraint in (4.5). $\square$

Theorem 4.3 provides an upper bound to the largest singular value of the error dynamics of the interconnected system $\bar{\sigma}(E_c(i\omega)) \leq \varepsilon_c^\star(\omega)$ introduced by reduction errors bounded by $\bar{\sigma}(E_j(i\omega)) \leq \varepsilon_j(\omega)$ for all $j \in \{1, \ldots, k\}$ at frequency ω. Similar to the global case, we can solve the problem (4.5) after several steps explained next. First, by setting $d_c = 1$, we can replace $W^F(\omega) D_r W^F(\omega)$ by

$$
diag\left(d_1 \varepsilon_1^2(\omega) I_{m_1}, \ldots, d_k \varepsilon_k^2(\omega) I_{m_2}, \frac{1}{\varepsilon_c^2(\omega)} I_{p_c}\right).
\tag{4.7}
$$

Then, after defining $\gamma := \varepsilon_c^{-2}(\omega)$, the inequalities in (4.5) are linear in the decision variables $d_1, \ldots, d_k$ and γ and the solution to problem (4.5) can be found using standard SDP solvers for any $\omega \in \mathbb{R}$. Note, also for this case, it holds that if no feasible solution can be found for some $\omega \in \mathbb{R}$, no conclusion on the existence of an upper bound on $\bar{\sigma}(E_c(i\omega))$ for that frequency can be made.

Remark 4.4. For the reduction of subsystems, model reduction methods such as balanced truncation can only provide global error bounds $\bar{\varepsilon}_j$ as shown by (2.9) in Remark 2.2. In this case, let $\varepsilon_j(\omega) = \bar{\varepsilon}_j$ for all $j \in \{1, \ldots, k\}$ for all $\omega \in \mathbb{R}$ using the given a priori error bounds on the subsystems $\bar{\varepsilon}_j$. However, μ-analysis is inherently frequency-dependent. Therefore, a frequency-dependent error bound on the interconnected system error dynamics $\varepsilon_c(\omega)$ can still be found by using Theorem 4.3. Note that, as we will show in Section 5, the conservativeness of $\varepsilon_c(\omega)$ is subject to the conservativeness the subsystem error bound $\bar{\varepsilon}_j$ provided.

4.2. Top-down approach: E_j specification based on E_c requirements

In this section, we show how Theorems 3.2 and 3.4 can be employed such that global and frequency-dependent reduction error specifications on E_j on a subsystem level can be directly computed from a reduction error E_c requirement on the interconnected system model. This approach allows for specifically tailored subsystem reduction that guarantees the required accuracy on the interconnected system model.

Remark 4.5. In the top-down approach, we assume that we have some reduction error bound requirement on the interconnected system, either a global bound $\bar{\varepsilon}_c$ or a frequency-dependent bound $\varepsilon_c(\omega)$. This bound can be defined from requirements on the accuracy of the interconnected system model. The goal in the general top-down approach is to find some set of either global $\bar{\varepsilon}_j$ or frequency-dependent $\varepsilon_j(\omega)$ reduction error bounds for all subsystems $j \in \{1, \ldots, k\}$ for which it can be guaranteed that reduction the error bound on the interconnected system will not be exceeded. In practice, there is an infinite number of possible combinations of $\bar{\varepsilon}_j$ (or $\varepsilon_j(\omega)$) that satisfy this requirement. Given the fact that there are many subsystem reduction options to achieve the required subsystem accuracy, finding some, in some sense, to be defined, (sub-)optimal distributions of $\bar{\varepsilon}_j$ and $\varepsilon_j(\omega)$ for now requires a heuristic approach. The development of a systematic approach to tackle this is still an open problem.

Within the scope of this paper, we assume that a global error specification $\bar{\varepsilon}_c$ on the reduction error dynamics of the interconnected system model is given. We then focus on restricting how E_q, the error of a single subsystem $j = q$ contributes to the error of the interconnected system E_c. This approach can be used for all subsystems individually, and therefore can be used to reduce all subsystems, but does not solve the problem of finding an optimal distribution between subsystem errors (see Remark 4.5). However, it is still a relevant problem, since it allows for the specification of reduction error bounds on a subsystem level, based on specifications on the desired accuracy of the overall interconnected system model.

Let reduction error bounds be given for all other reduced-order subsystems, i.e., $\|E_j\|_\infty \leq \bar{\varepsilon}_j, j \neq q$. Then, we aim to find the maximum to a global error bound $\bar{\varepsilon}_q$ such that E_c is guaranteed to be stable and the global error specification $\bar{\varepsilon}_c$ for the interconnected system is satisfied using the following theorem.

Theorem 4.6. Let $\bar{\varepsilon}_c > 0$ be given. Let $E_j \in \mathcal{RH}_\infty$ and let $\bar{\varepsilon}_j$ such that $\|E_j\|_\infty \leq \bar{\varepsilon}_j$ for all $j \neq q$. Consider the optimization problem

$$
\begin{aligned}
&\text{given} && \bar{\varepsilon}_c, \bar{\varepsilon}_j, j \neq q \\
&\underset{D_\ell, D_r, W^G}{\text{maximize}} && \bar{\varepsilon}_q \\
&\text{subject to} && N(i\omega)W^G D_r W^G N^H(i\omega) \prec D_\ell \; \forall \; \omega, \\
&&& (D_\ell, D_r) \in \mathbf{D} && (4.8)
\end{aligned}
$$

with $W^G := diag(\bar{\varepsilon}_1 I_{m_1}, \ldots, \bar{\varepsilon}_k I_{m_k}, \bar{\varepsilon}_c^{-1} I_{p_c})$ and $\mathbf{D}$ as in (3.17). If $\bar{\varepsilon}_q^\star$ is a feasible solution to (4.8), then for all $E_q \in \mathcal{RH}_\infty$ such that $\|E_q\|_\infty \leq \bar{\varepsilon}_q^\star$, we have

 (1) E_c is well-posed,
 (2) E_c is internally stable, and
 (3) $\|E_c\|_\infty < \bar{\varepsilon}_c^\star$.

Proof. The proof follows directly from the proof of Theorem 4.1. □

Theorem 4.6 guarantees that if $\bar{\varepsilon}_q^\star$ exists, all error dynamics E_q introduced by reduction of subsystem q satisfying $\|E_q\| \leq$

$\bar{\varepsilon}_q^\star$ result in stable interconnected system model reduction error dynamics bounded by $\|E_c\|_\infty < \bar{\varepsilon}_c$. The problem (4.8) can be simplified similar to the global bottom-up problem as in (4.1). Here, we set $d_q = 1$ and set $\gamma := \bar{\varepsilon}_q^2$. Then, the inequality in (4.8) is linear for the decision variables d_c, d_j for all $j \neq q$, and γ and maximizing γ using SDP gives a maximum global upper bound on the (allowed) subsystem error dynamics $\|E_q\|_\infty \leq \bar{\varepsilon}_q$. If some reduced-order subsystem $\hat{G}_q$ is found for which the upper bound $\bar{\varepsilon}_q$ is satisfied, Theorem 4.6 guarantees that $\|E_c\|_\infty \leq \bar{\varepsilon}_c$.

This top-down problem is easily translated to a frequency-dependent problem using Theorem 3.4. Namely, we consider some frequency-dependent error specification $\varepsilon_c(\omega)$ for which we can guarantee that $\bar{\sigma}(E_c(i\omega)) \leq \varepsilon_c(\omega)$. Additionally, we assume that some subsystem error bound $\bar{\sigma}(E_j(i\omega)) \leq \varepsilon_j(\omega)$ of all subsystems $j \neq q$ is known. Then, we aim to find a frequency-dependent error specification $\varepsilon_q(\omega)$ for which it holds that $\bar{\sigma}(E_q(i\omega)) \leq \varepsilon_q(\omega)$ using the following theorem that can be applied to any (discrete set of frequencies) $\omega \in \mathbb{R}$.

Theorem 4.7. Let ω in $\mathbb{R}$. Let $\varepsilon_j(\omega)$ be such that $\bar{\sigma}(E_j(i\omega)) \leq \varepsilon_j(\omega)$ for all $j \neq q$. Consider the optimization problem

$$
\begin{aligned}
&\text{given} && \varepsilon_c(\omega), \varepsilon_j(\omega), j \neq q \\
&\underset{D_\ell, D_r, W^F(\omega)}{\text{maximize}} && \varepsilon_q(\omega) \\
&\text{subject to} && N(i\omega)W^F(\omega)D_r W^F(\omega)N^H(i\omega) \prec D_\ell, \\
&&& (D_\ell, D_r) \in \mathbf{D} && (4.9)
\end{aligned}
$$

with $W^F(\omega) := diag(\varepsilon_1(\omega)I_{m_1}, \ldots, \varepsilon_k(\omega)I_{m_k}, \varepsilon_c^{-1}(\omega)I_{p_c})$ and $\mathbf{D}$ as in (3.17). If $\varepsilon_q^\star(\omega)$ is a feasible solution to (4.9), then for all E_q such that $\bar{\sigma}(E_q(i\omega)) \leq \varepsilon_q^\star(\omega)$, we have $\bar{\sigma}(E_c(i\omega)) < \varepsilon_c(\omega)$.

Proof. The proof follows directly from the proof of Theorem 4.3. □

Theorem 4.7 guarantees that if $\varepsilon_q^\star(\omega)$ exists for ω, then any error dynamics at $E_q(i\omega)$ introduced by reduction of subsystem q satisfying $\bar{\sigma}(E_q(i\omega)) \leq \varepsilon_q^\star(\omega)$ results in interconnected system error dynamics bounded by $\bar{\sigma}(E_c(i\omega)) < \varepsilon_c(\omega)$ at frequency ω.

The problem (4.9) can be simplified similar to the frequency-dependent bottom-up problem as in (4.5). Here, we set $d_q = 1$ and set $\gamma := \varepsilon_q^2(\omega)$. Then, problem (4.9) is linear for the decision variables d_c, d_j for all $j \neq q$, and γ and maximizing γ using SDP for any $\omega \in \mathbb{R}$ gives a frequency-dependent upper bound on the subsystem error dynamics $\bar{\sigma}(E_q(i\omega)) \leq \varepsilon_q(\omega)$. If some reduced-order subsystem $\hat{G}_q$ is found for which this upper bound is satisfied, Theorem 4.7 guarantees that $\bar{\sigma}(E_c(i\omega)) \leq \varepsilon_c(\omega)$. By computing (4.5) over a frequency grid, this guarantee holds for the $\omega \in \mathbb{R}$ of interest.

Remark 4.8. For the top-down approach, a frequency-dependent error bound $\bar{\sigma}(E_c(i\omega)) \leq \varepsilon_c(\omega)$ can be defined by the user based on requirements on the interconnected model accuracy. This allows for the flexibility to design specifications on the interconnected system such that the reduced-order system is accurate in frequencies ranges that are relevant for the way the model is used. If the reduced-order interconnected system model needs to be especially accurate in a certain frequency range, the error requirement $\varepsilon_c(\omega)$ can be chosen low in this frequency range, enforcing a higher accuracy in this frequency range. After applying the top-down approach, meeting the specification of frequency-dependent error bounds on subsystem level $\bar{\sigma}(E_q(i\omega)) \leq \varepsilon_q(\omega)$ guarantees accuracy around this frequency.

In this section, we have given several approaches to compute a relation between bounds on E_j and E_c using μ-analysis. To properly illustrate how these approaches can be useful for modular

Parameter	Subsys. 1	Subsys. 2	Subsys. 3
Cross-sect. area [m^2]	1×10^{-5}	1×10^{-5}	1×10^{-5}
2nd area moment [m^4]	1×10^{-9}	1×10^{-9}	1×10^{-9}
Young's modulus [Pa]	2×10^{11}	2×10^{11}	2×10^{11}
Mass density [kg/m^3]	8×10^3	8×10^3	8×10^3
Modal damping [–]	0.06	0.06	0.06
Length [m]	1	0.4	0.6
# of elements [–]	100	40	60
Transfer function	$G_1(s)$	$G_2(s)$	$G_3(s)$
# of states n_j [–]	400	164	240
# of inputs m_j [–]	2	5	2
# of outputs p_j [–]	2	4	3

Fig. 6. Example system: two cantilever beams (Subsystems 1 and 3) connected on their free ends to a free-free beam (Subsystem 2) with translational and rotational springs.

model reduction of systems of interconnected LTI systems, in the next section, an illustrative example from structural dynamics on which these approaches are applied will be discussed.

5. Illustrative example

To illustrate the proposed framework for error analysis of modular model reduction of interconnected systems, we apply it to a mechanical system consisting of three interconnected beams as illustrated schematically in Fig. 6. Subsystems 1 and 3 are cantilever beams which are connected on their free ends to free-free beam 2 with translational and rotational springs. The stiffness of both translational interconnecting springs is $k_1^t = k_2^t = 4 \times 10^4$ N/m. The stiffness of both rotational interconnecting springs is $k_1^r = k_2^r = 4 \times 10^2$ Nm/rad. The interconnection structure matrix K in (2.2) is therefore given by

$$K = \begin{bmatrix} -k_1^t & 0 & k_1^t & 0 & 0 & 0 & 0 & 0 & 0 & 0 \\ 0 & -k_1^r & 0 & k_1^r & 0 & 0 & 0 & 0 & 0 & 0 \\ k_1^t & 0 & -k_1^t & 0 & 0 & 0 & 0 & 0 & 0 & 0 \\ 0 & k_1^r & 0 & -k_1^r & 0 & 0 & 0 & 0 & 0 & 0 \\ 0 & 0 & 0 & 0 & 0 & 0 & 0 & 0 & 0 & 1 \\ 0 & 0 & 0 & 0 & -k_2^t & 0 & k_2^t & 0 & 0 & 0 \\ 0 & 0 & 0 & 0 & 0 & -k_2^r & 0 & k_2^r & 0 & 0 \\ 0 & 0 & 0 & 0 & k_2^t & 0 & -k_2^t & 0 & 0 & 0 \\ 0 & 0 & 0 & 0 & 0 & k_2^r & 0 & -k_2^r & 0 & 0 \\ 0 & 0 & 0 & 0 & 0 & 0 & 0 & 0 & 1 & 0 \end{bmatrix}.$$

$$(5.1)$$

The external input force u_c [N] is applied to the middle of subsystem 2 in the transversal direction. The external output displacement y_c [m] is measured at the middle of subsystem 3 in the transversal direction.

Each beam/subsystem is discretized by linear two-node Euler beam elements (only bending, no shear, see Craig and Kurdila (2006)) of equal length. Per node we have one translational degree of freedom (dof), i.e., a transversal displacement, and one rotational dof. For each beam, viscous damping is modelled using 6% modal damping. Physical and geometrical parameter values of the three beams and information about finite element discretization, the number of states and the number of subsystem inputs and outputs are given in Table 1. With this information we can construct $G_1(s)$, $G_2(s)$ and $G_3(s)$ and the interconnected system $G_c(s)$ is then given according to Section 2 where $k = 3$ and K is defined by 5.1.

Below, both the bottom-up and the top-down approaches from Section 4 are concisely illustrated. First, in Section 5.1, we consider a bottom-up problem in which we show how the error
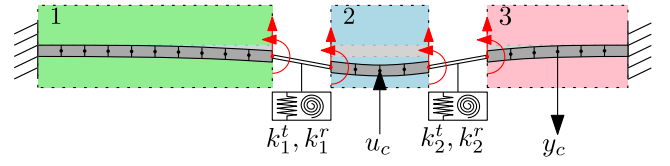
in the interconnected system introduced by the reduction of subsystem 1 can be bounded first by using a global error bound and then by using a frequency-dependent error bound. Subsequently, in Section 5.2, we show how specifications on the accuracy of the reduced-order interconnected system can be translated to frequency-dependent bounds on the reduction error of subsystem 1 and how this information can be used to find a ROM that takes this frequency-dependent bound into account.

5.1. Bottom-up approach

In the bottom-up approach, we use Theorems 4.1 and 4.3 to find both global and frequency-dependent a priori bounds on the reduction error of the interconnected system model shown in Fig. 6. Note that in this example, subsystem 1 is reduced using balanced truncation (Antoulas, 2005) to find some $\hat{G}_1(s)$ whereas the models of subsystems 2 and 3 are left unreduced.

First, we consider two types of errors on E_1:

(1) A priori error bounds $\|E_1\|_\infty \leq \bar{\varepsilon}_1$ using the Hankel singular values as in (2.9).
(2) The actual $\mathcal{H}_\infty$-norm of the error dynamics $\|E_1\|_\infty = \bar{\varepsilon}_{1,a}$, determined after the reduction of the subsystem.

Remark 5.1. Note that $\bar{\varepsilon}_1$ is used to determine a priori error bounds $\bar{\varepsilon}_c$ on the interconnected system. However, these a priori error bounds already have some conservativeness on a subsystem level. The gap between $\bar{\varepsilon}_{c,a}$ and $\bar{\varepsilon}_c$ indicates how much of conservativeness of $\bar{\varepsilon}_c$ is attributed to the conservativeness of $\bar{\varepsilon}_1$.

These errors are computed for varying values of the reduced-order r_1 of subsystem 1. Second, the bottom-up SDP problem in Theorem 4.1 is solved for the resulting values for $\bar{\varepsilon}_1$ and $\bar{\varepsilon}_{1,a}$. The solution to these SDPs provides an error bound $\|E_c\|_\infty \leq \bar{\varepsilon}_c$ and $\|E_c\|_\infty \leq \bar{\varepsilon}_{c,a}$ for $\bar{\varepsilon}_1$ and $\bar{\varepsilon}_{1,a}$, respectively. Additionally, to compare the method to the existing a priori error bound for such systems, $\|E_c\|_\infty \leq \bar{\varepsilon}_{c,\text{Reis}}$ from Reis and Stykel (2007, Theorem 3.1) is computed. Finally, to compare how conservative the error bounds are with respect to different orders of reduction, $\bar{\varepsilon}_{c,a}/\|E_c\|_\infty$ and $\bar{\varepsilon}_c/\|E_c\|_\infty$ are determined. The results are given in Table 2.

Remark 5.2. Note that the actual $\|E_c\|_\infty$ can only be computed a posteriori (so after the reduction has been pursued and the reduced-order interconnected system has been constructed). We emphasize that the methodology in this paper allows to compute the bounds for $\|E_c\|_\infty$ a priori.

From Table 2, we can make several observations. Solving the bottom-up SDP problem in Theorem 4.1 provides an a priori global error bound on the error dynamics of the interconnected system $\|E_c\|_\infty$ using global error bounds on subsystem level. Additionally, for the $\mathcal{H}_\infty$-norm of the actual error dynamics $\bar{\varepsilon}_{c,a}$, the bottom-up approach provides tight(er) error bounds on the level of the interconnected system, as indicated by the small values of $\bar{\varepsilon}_{c,a}/\|E_c\|_\infty$. In contrast, since the values of $\bar{\varepsilon}_c/\|E_c\|_\infty$ are clearly

Table 2

Bottom-up global error bounds example: comparison between $\|E_c\|_\infty \leq \bar{\varepsilon}_{c,a} \leq \bar{\varepsilon}_c$ and $\bar{\varepsilon}_{c,\text{Reis}}$ for a different number of states r_1 in the reduced-order subsystem $\hat{G}_1$. To show conservativeness of the error bounds, $\bar{\varepsilon}_{c,a}/\|E_c\|_\infty$, $\bar{\varepsilon}_c/\|E_c\|_\infty$ and $\bar{\varepsilon}_{c,\text{Reis}}/\|E_c\|_\infty$ are given. $\bar{\varepsilon}_1/\|E_1\|_\infty$ shows the conservativeness present in the a priori error bound on subsystem level. If no error bound could be found, the result is denoted with "–".

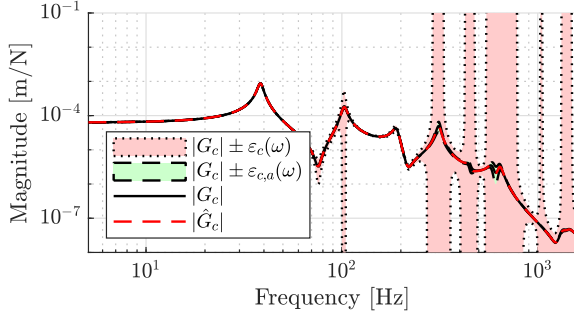| r_1 [–]	Actual error	Error bounds			Conservativeness factor			
	$\|E_c\|_\infty$ [m/N]	$\bar{\varepsilon}_{c,a}$ [m/N]	$\bar{\varepsilon}_c$ [m/N]	$\bar{\varepsilon}_{c,\text{Reis}}$ [m/N]	$\frac{\bar{\varepsilon}_{c,a}}{\|E_c\|_\infty}$	$\frac{\bar{\varepsilon}_c}{\|E_c\|_\infty}$	$\frac{\bar{\varepsilon}_{c,\text{Reis}}}{\|E_c\|_\infty}$	$\frac{\bar{\varepsilon}_1}{\|E_1\|_\infty}$
400 (n_1)	0	0	0	0	–	–	–	–
140	2.59×10^{-9}	3.52×10^{-9}	1.03×10^{-7}	9.31×10^{-4}	1.36	40.0	3.60×10^5	2.25
120	5.01×10^{-9}	6.02×10^{-9}	5.74×10^{-7}	5.12×10^{-3}	1.20	115	1.02×10^6	6.46
100	1.89×10^{-8}	2.90×10^{-8}	3.43×10^{-6}	–	1.53	181	–	99.2
80	4.32×10^{-8}	1.18×10^{-7}	3.46×10^{-5}	–	2.73	801	–	163
60	9.04×10^{-8}	5.44×10^{-7}	–	–	6.01	–	–	223
40	2.19×10^{-6}	2.30×10^{-5}	–	–	10.5	–	–	56.0
20	1.00×10^{-4}	–	–	–	–	–	–	9.25

Fig. 7. Bottom-up approach: Magnitude plot for the high-order interconnected system $|G_c(i\omega)|$, the reduced-order interconnected system $|\hat{G}_c(i\omega)|$ with $r_1 = 60$, the a priori error bound using a priori frequency-dependent subsystem errors $|G_c(i\omega)| \pm \varepsilon_c(\omega)$ and the frequency-dependent error bound using the largest singular values of the actual subsystem error $|G_c(i\omega)| \pm \varepsilon_{c,a}(\omega)$. (For interpretation of the references to colour in this figure legend, the reader is referred to the web version of this article.)
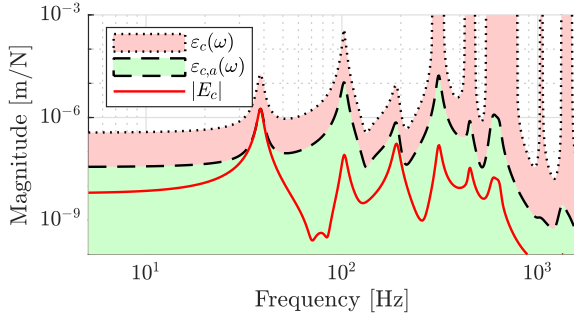

Fig. 8. Bottom-up approach: Magnitude plot for the interconnected system error dynamics $|E_c(i\omega)|$ with $r_1 = 60$, the a priori frequency-dependent error bound using a priori subsystem errors $\varepsilon_c(\omega)$ and the frequency-dependent error bound using the largest singular values of the actual subsystem error $\varepsilon_{c,a}(\omega)$. (For interpretation of the references to colour in this figure legend, the reader is referred to the web version of this article.)

higher, the error bound using the a priori errors on the subsystem level $\|E_1\|_\infty \leq \bar{\varepsilon}_1$ is significantly more conservative. However, the subsystem a priori error bound $\bar{\varepsilon}_1$ already provides some level of conservativeness, as indicated by the values of $\bar{\varepsilon}_1/\|E_1\|_\infty$. Therefore, we postulate that the conservativeness of the a priori error bound $\bar{\varepsilon}_c/\|E_c\|_\infty$ is for a significant part attributed to the conservativeness of $\bar{\varepsilon}_1/\|E_1\|_\infty$. Additionally, in comparison with the existing a priori error bound from Reis and Stykel (2007), $\bar{\varepsilon}_c$ is significantly less conservative, i.e., for $r_1 = 140$ and $r_1 = 120$, $\bar{\varepsilon}_{c,\text{Reis}}$ is around 10^4 times more conservative, and it is not available for $r_1 \leq 100$.

As can be seen in Table 2, for this example, no global a priori error bound $\bar{\varepsilon}_c$ can be found for a reduction of $r_1 \leq 60$

using Theorem 4.1 with $\bar{\varepsilon}_1$. However, although no global error bound on E_c can be found for significant reduction of subsystem 1, frequency-dependent bounds can still be found for intervals $\omega \in \mathbb{R}$. Below, we show how Theorem 4.3 can be used to find frequency-dependent error bounds on E_c. Frequency-dependent error bounds can be computed to provide useful insights on how reduction errors on the subsystem level propagate to the interconnected system.

First, we compute a reduced-order model $\hat{G}_1$ for subsystem 1 using balanced truncation with $r_1 = 60$. Then, we consider and calculate two types of errors on $E_1(s)$:

(1) The same a priori error bounds $\|E_1\|_\infty \leq \bar{\varepsilon}_1$ as in the global case (see Remark 4.4).
(2) Frequency-dependent error bounds $\varepsilon_{1,a}(\omega)$ as the largest singular value of the actual error dynamics $\bar{\sigma}(E_1(i\omega)) = \varepsilon_{1,a}(\omega)$, determined after the reduction of the subsystem.

Second, the bottom-up SDP problem in Theorem 4.3 is solved for the resulting values for $\varepsilon_1(\omega) = \bar{\varepsilon}_1$ and $\varepsilon_{1,a}(\omega)$. The solution to these SDPs provides an error bound $\bar{\sigma}(E_c(i\omega)) \leq \varepsilon_c(\omega)$ and $\bar{\sigma}(E_c(i\omega)) \leq \varepsilon_{c,a}(\omega)$ for each $\varepsilon_1(\omega) = \bar{\varepsilon}_1$ and $\varepsilon_{1,a}(\omega)$, respectively, as shown in Figs. 7 and 8.

From these figures, we can make several observations. In Figs. 7 and 8, in the green areas, the frequency-dependent a priori error bound $\varepsilon_{c,a}(\omega)$ (based on $\varepsilon_{1,a}(\omega)$) is found for all frequencies in the shown domain. In Fig. 8, it can be clearly seen that this bound is particularly tight. Therefore, in Fig. 7, the effect of $\varepsilon_{c,a}(\omega)$ is not even visible. Additionally, it can be seen in the red areas, which illustrate the frequency-dependent a priori error bound $\varepsilon_c(\omega)$, that for several frequencies in the shown domain, no bound $\varepsilon_c(\omega)$ is found. This is in agreement with Table 2, where the bottom-up approach indeed cannot find a global a priori error bound $\varepsilon_c(\omega)$ for $r_1 = 60$. However, for most other frequencies, an a priori error bound $\varepsilon_c(\omega)$ can still be computed. In total, both ε_c and $\varepsilon_{c,a}$ give a clear frequency-dependent reduction error bound for the largest part of the frequency domain, which can be used to give a frequency-dependent upper bound on how substructure reduction errors propagate to the interconnected system, even when no global error bound can be found. The inverse of this problem, finding an upper bound on subsystem errors based on requirements on the interconnected system, is shown on the same system in the next section.

5.2. Top-down approach

In this example, the top-down approach using the optimization problem in Theorem 4.7 is applied to the example system in Fig. 6. Specifically, a required frequency-dependent reduction error bound $\bar{\sigma}(E_1(i\omega)) \leq \varepsilon_1(\omega)$ for subsystem 1 is computed that guarantees a user-selected frequency-dependent error bound $\bar{\sigma}(E_c(i\omega)) \leq \varepsilon_c(\omega)$ on the interconnected system. Additionally,
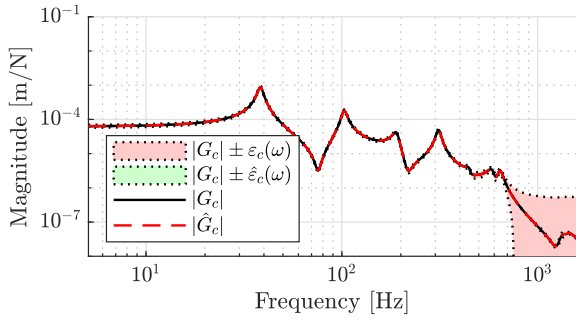
Fig. 9. Top-down approach: Magnitude plot for the high-order interconnected system $|G_c(i\omega)|$, the reduced-order interconnected system $|\hat{G}_c(i\omega)|$ with $r_1 = 20$, the a priori frequency-dependent error bound using the actual subsystem error bounds $|G_c(i\omega)| \pm \hat{\varepsilon}_c(\omega)$ and the user defined frequency-dependent error bound $|G_c(i\omega)| \pm \varepsilon_c(\omega)$. (For interpretation of the references to colour in this figure legend, the reader is referred to the web version of this article.)
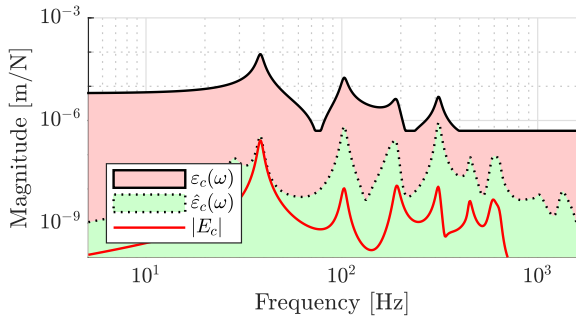

Fig. 10. Top-down approach: Magnitude plot for the high-order interconnected error dynamics $|E_c(i\omega)|$ with $r_1 = 20$, the frequency-dependent error bound using the actual subsystem errors $\hat{\varepsilon}_c(\omega)$ and the user defined frequency-dependent error bound $\varepsilon_c(\omega)$. (For interpretation of the references to colour in this figure legend, the reader is referred to the web version of this article.)
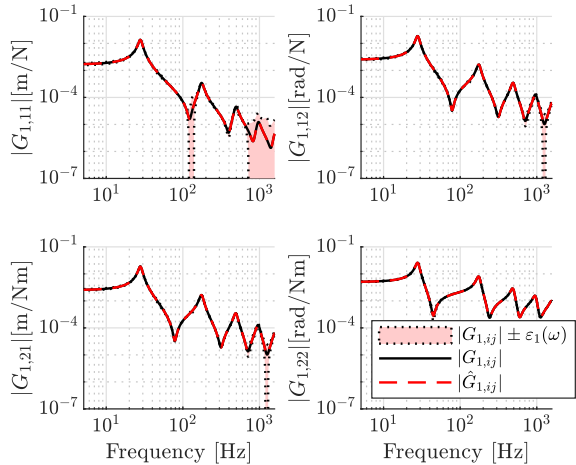

Fig. 11. Top-down approach: Magnitude plot of the high-order subsystem $|G_{1,ij}(i\omega)|$, the reduced-order subsystem $|\hat{G}_{1,ij}(i\omega)|$ with $r_1 = 20$ and the allowed frequency-dependent error with the top-down approach $|G_{1,ij}(i\omega)| \pm \varepsilon_1(\omega)$ from input i to output j. (For interpretation of the references to colour in this figure legend, the reader is referred to the web version of this article.)

a reduced-order subsystem $\hat{G}_1(s)$ is computed that meets these requirements. Recall that subsystems 2 and 3 remain unreduced, i.e., $\bar{\varepsilon}_2 = \varepsilon_2(\omega) = \bar{\varepsilon}_3 = \varepsilon_3(\omega) = 0$. The computation of $\hat{G}_1(s)$ serves two purposes. Namely, (1) to validate the results, and (2) to show how frequency-weighted balanced truncation can exploit
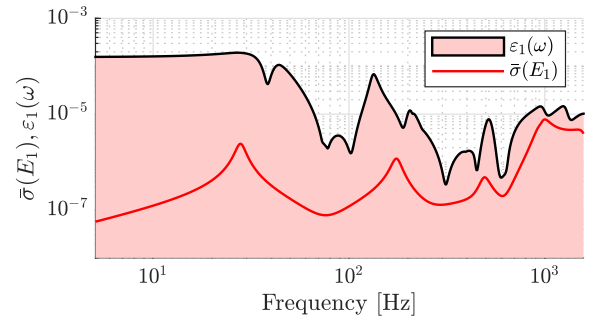

Fig. 12. Top-down approach: Largest singular value plot of the high-order subsystem error dynamics $\bar{\sigma}(E_1(i\omega))$ with $r_1 = 20$ and the allowed frequency-dependent error found using the top-down approach $\varepsilon_1(\omega)$. (For interpretation of the references to colour in this figure legend, the reader is referred to the web version of this article.)

the frequency information in the error bounds to increase the amount of reduction that can be achieved.

Remark 5.3. Note that any reduced-order subsystem $\hat{G}_1(s)$ for which $\bar{\sigma}(E_1(i\omega)) \leq \varepsilon_1(\omega)$ holds for the specified frequencies can be used, regardless of the model reduction method. Frequency-weighted balanced truncation is a special form of balanced truncation in which the goal is to reduce the frequency-weighted error between $G(s)$ and $\hat{G}(s)$ (Gugercin & Antoulas, 2004). This method is particularly suitable for the top-down approach since it allows to capitalize on the computed frequency-dependent error bound $\varepsilon_1(\omega)$ for the reduction of the subsystem. Specifically, we can directly apply the computed W^F in Theorem 4.7 as a weighting for the reduction. In this example, we use Enns' method (Enns, 1984) to minimize $\|W_1^F E_1\|_\infty$ (whereas regular balanced truncation minimizes $\|E_1\|_\infty$).

The top-down approach is applied in this example by carrying out the following steps:

(1) All frequencies ω over a grid of 1000 logarithmically spaced points in the interval $[10^{1.5}, 10^4]$ rad/s are evaluated. For these frequencies, a frequency-dependent error bound $\varepsilon_c(\omega)$ is defined, as can be done by the user (see Remark 4.8). In this example, this bound is chosen as some fraction β_1 of the magnitude of $\bar{\sigma}(G_c(i\omega))$, bounded below by β_2, given as

$$\varepsilon_c(\omega) = \max\{\beta_1 \cdot \bar{\sigma}(G_c(i\omega)), \beta_2\}, \tag{5.2}$$

where $\beta_1 = 0.1$ and $\beta_2 = 5 \times 10^{-7}$ in this example. In Figs. 9 and 10, this bound $\varepsilon_c(\omega)$ is indicated by the red areas.

(2) The SDP problem in Theorem 4.7 is solved using $\varepsilon_c(\omega)$ with $q = 1$ to find some frequency-dependent error bound $\varepsilon_1(\omega)$ on the error dynamics of the first subsystem. Note that we assume unreduced subsystems 2 and 3, and therefore $\varepsilon_2(\omega) = \varepsilon_3(\omega) = 0$. The error bound $\varepsilon_1(\omega)$ corresponding to $\varepsilon_c(\omega)$ is indicated by the red areas in Figs. 11 and 12.

(3) A reduced-order subsystem $\hat{G}_1$ with $r_1 = 20$ is found using frequency-weighted balanced truncation (see Remark 5.3) for which $\bar{\sigma}(E_1(i\omega)) \leq \varepsilon_1(\omega)$ holds, as shown by the red lines in Figs. 11 and 12.

(4) For validation, the bottom-up approach as given in Theorem 4.3 is solved to find some a priori worst-case upper bound on the interconnected system error dynamics $\bar{\sigma}(E_c(i\omega)) \leq \hat{\varepsilon}_c(\omega)$ caused by the replacement of G_1 by $\hat{G}_1$ in the interconnected system. In Figs. 9 and 10, this bound $\hat{\varepsilon}_c(\omega)$ is indicated by the green areas.

(5) As additional validation, the reduced-order interconnected system $\hat{G}_c$ and the error dynamics E_c are computed and shown by the red line in Figs. 9 and 10, which are indeed fully within the red and green areas.

Remark 5.4. Note that in theory, if $\bar{\sigma}(E_1(i\omega))$ would match the allowed error bound $\varepsilon_1(\omega)$ in Fig. 12, we would see that $\hat{\varepsilon}_c(\omega) = \varepsilon_c(\omega)$ in Fig. 10. However, after reduction, Fig. 12 shows that the largest singular values $\bar{\sigma}(E_1(i\omega))$ of the reduced-order subsystem 1 do not fully "utilize" the allowed error $\varepsilon_1(\omega)$. As a result, in Fig. 10, we can see that $\hat{\varepsilon}_c(\omega)$ is much smaller than $\varepsilon_c(\omega)$. Therefore, the distance between $|E_c(i\omega)|$ and $\varepsilon_c(\omega)$ in Fig. 10 is a combination between the conservativeness of the top-down approach, given by the gap in $|E_c(i\omega)| < \hat{\varepsilon}_c(\omega)$, and the fact that $\bar{\sigma}(E_1(i\omega)) \leq \varepsilon_1(\omega)$, which results in the gap in $\hat{\varepsilon}_c(\omega) \leq \varepsilon_c(\omega)$.

In summary, this example shows that the top-down approach can be effectively used to find subsystem 1 error bounds given some interconnected system accuracy specification. This translation from requirements on the interconnected system to requirements on a subsystem level is particularly useful because (1) any reduced-order subsystem model that satisfies the bounds is guaranteed not to cause the error in the interconnected system to exceed the required accuracy, and (2) a reduced-order subsystem model can be developed by making use of the frequency-dependent error bound, in this case using frequency-weighted balanced truncation (see Remark 5.3), to further reduce the interconnected system model.

6. Conclusions

Modular model reduction is a computationally efficient method that allows for the computation of ROMs of interconnected (multidisciplinary and multi-physical) subsystems. However, generally, modular model reduction leads to less accurate ROMs of the interconnected system in comparison to costly direct (structure-preserving) reduction methods. In this paper, to mitigate this accuracy disadvantage, a mathematical relation between the accuracy of reduced subsystem models and the accuracy of the reduced interconnected system model is introduced.

The main idea relies on defining the error dynamics introduced by the MOR of a subsystem as a block-diagonal structured uncertainty. Then, the system can be reformulated into the framework of a robust performance problem. This allows for a direct computation of a relation between upper bounds of subsystem reduction error dynamics to upper bounds on the interconnected system reduction error dynamics using the structured singular value μ.

This relation can then be used in the two ways. (1) a bottom-up approach can be used to guarantee stability of the interconnected, reduced-order system and determine (frequency-dependent) a priori error bounds for interconnected system model reduction when a priori error bounds are available for the reduced subsystem models. (2) a top-down approach allows the user to define (frequency-dependent) accuracy specifications on the reduced interconnected system model. These specifications can then be translated to (frequency-dependent) accuracy requirements on reduced subsystem models. When these are achieved, they guarantee that the user-defined specifications on the interconnected system hold. Additionally, this allows for the effective use of frequency-weighted balanced truncation to achieve reduction of the subsystem while guaranteeing that the interconnected system accuracy specifications are met and remains stable. To demonstrate the use of these approaches, they have been applied to a structural dynamics beam system.

References

Antoulas, A. C. (2005). *Approximation of large-scale dynamical systems*. SIAM, Philadelphia.

Benner, P., Gugercin, S., & Willcox, K. (2015). A survey of projection-based model reduction methods for parametric dynamical systems. *SIAM Review*, *57*(4), 483–531.

Besselink, B., Sandberg, H., & Johansson, K. H. (2015). Clustering-based model reduction of networked passive systems. *IEEE Transactions on Automatic Control*, *61*(10), 2958–2973.

Besselink, B., Tabak, U., Lutowska, A., Van de Wouw, N., Nijmeijer, H., Rixen, D. J., et al. (2013). A comparison of model reduction techniques from structural dynamics, numerical mathematics and systems and control. *Journal of Sound and Vibration*, *332*(19), 4403–4422.

Boyaval, S., Le Bris, C., Lelievre, T., Maday, Y., Nguyen, N. C., & Patera, A. T. (2010). Reduced basis techniques for stochastic problems. *Archives of Computational Methods in Engineering*, *17*(4), 435–454.

Boyd, S., Balakrishnan, V., & Kabamba, P. (1989). A bisection method for computing the H∞ norm of a transfer matrix and related problems. *Mathematics of Control, Signals, and Systems*, *2*(3), 207–219.

Bruinsma, N. A., & Steinbuch, M. (1990). A fast algorithm to compute the H∞-norm of a transfer function matrix. *Systems & Control Letters*, *14*(4), 287–293.

Buhr, A., & Smetana, K. (2018). Randomized local model order reduction. *SIAM Journal on Scientific Computing*, *40*(4), A2120–A2151. http://dx.doi.org/10.1137/17M1138480.

Cheng, X., & Scherpen, J. M. A. (2021). Model reduction methods for complex network systems. *Annual Review of Control, Robotics, and Autonomous Systems*, *4*, 425–453.

Craig, R., Jr. (2000). Coupling of substructures for dynamic analyses-an overview. In *41st structures, structural dynamics, and materials conference and exhibit* (p. 1573).

Craig, R. R., Jr., & Kurdila, A. J. (2006). *Fundamentals of structural dynamics*. Hoboken, N.J.: John Wiley & Sons, ISBN: 9781118174814.

de Klerk, D., Rixen, D. J., & Voormeeren, S. N. (2008). General framework for dynamic substructuring: history, review and classification of techniques. *American Institute of Aeronautics and Astronautics*, *46*(5), 1169–1181.

Enns, D. F. (1984). Model reduction with balanced realizations: An error bound and a frequency weighted generalization. In *Proceedings of the 23rd IEEE conference on decision and control* (pp. 127–132). IEEE.

Glover, K. (1984). All optimal Hankel-norm approximations of linear multivariable systems and their L∞-error bounds. *International Journal of Control*, *39*(6), 1115–1193.

Grimme, E. J. (1997). *Krylov projection methods for model reduction* (Ph.D. thesis), University of Illinois at Urbana-Champaign.

Gugercin, S., & Antoulas, A. C. (2004). A survey of model reduction by balanced truncation and some new results. *International Journal of Control*, *77*(8), 748–766.

Ishizaki, T., Kashima, K., Imura, J., & Aihara, K. (2013). Model reduction and clusterization of large-scale bidirectional networks. *IEEE Transactions on Automatic Control*, *59*(1), 48–63.

Janssen, L. A. L., Besselink, B., Fey, R. H. B., Hossein Abbasi, M., & van de Wouw, N. (2022). A priori error bounds for model reduction of interconnected linear systems using robust performance analysis. In *2022 American control conference* (pp. 1867–1872). http://dx.doi.org/10.23919/ACC53348.2022.9867830.

Kerschen, G., Golinval, J. C., Vakakis, A. F., & Bergman, L. A. (2005). The method of proper orthogonal decomposition for dynamical characterization and order reduction of mechanical systems: An overview. *Nonlinear Dynamics*, *41*(1), 147–169.

Krattiger, D., Wu, L., Zacharczuk, M., Buck, M., Kuether, R. J., Allen, M. S., et al. (2019). Interface reduction for Hurty/Craig-Bampton substructured models: Review and improvements. *Mechanical Systems and Signal Processing*, *114*, 579–603.

Lutowska, A. (2012). *Model order reduction for coupled systems using low-rank approximations* (Ph.D. thesis), Eindhoven University of Technology.

Moore, B. (1981). Principal component analysis in linear systems: Controllability, observability, and model reduction. *IEEE Transactions on Automatic Control*, *26*(1), 17–32.

Packard, A., & Doyle, J. C. (1993). The complex structured singular value. *Automatica*, *29*(1), 71–109.

Reis, T., & Stykel, T. (2007). Stability analysis and model order reduction of coupled systems. *Mathematical and Computer Modelling of Dynamical Systems*, *13*(5), 413–436.

Reis, T., & Stykel, T. (2008). A survey on model reduction of coupled systems. In *Model order reduction: Theory, research aspects and applications* (pp. 133–155). Springer, Berlin.

Sandberg, H., & Murray, R. M. (2009). Model reduction of interconnected linear systems. *Optimal Control Applications & Methods*, *30*(3), 225–245.

Schilders, W. H. A., & Lutowska, A. (2014). A novel approach to model order reduction for coupled multiphysics problems. In *Reduced order methods for modeling and computational reduction* (pp. 1–49). Springer.

Schilders, W. H. A., Van der Vorst, H. A., & Rommes, J. (2008). *Model order reduction: Theory, research aspects and applications.* Springer, Berlin.

Skogestad, S., & Postlethwaite, I. (2005). *Multivariable feedback control: Analysis and design.* John Wiley & Sons, Chichester.

Vandendorpe, A., & van Dooren, P. (2008). Model reduction of interconnected systems. In *Model order reduction: Theory, research aspects and applications* (pp. 305–321). Springer, Berlin.

Vaz, A. F., & Davison, E. J. (1990). Modular model reduction for interconnected systems. *Automatica*, *26*(2), 251–261.

Veldman, D. W. M., Fey, R. H. B., Zwart, H. J., van de Wal, M. M. J., van den Boom, J. D. B. J., & Nijmeijer, H. (2018). Semi-analytic approximation of the temperature field resulting from moving heat loads. *International Journal of Heat and Mass Transfer, 122*, 128–137.

Yeung, E., Goncalves, J., Sandberg, H., & Warnick, S. (2009). Network structure preserving model reduction with weak a priori structural information. In *Proceedings of the 48h IEEE conference on decision and control (CDC) held jointly with 2009 28th chinese control conference* (pp. 3256–3263). IEEE.

Young, P. M., Newlin, M. P., & Doyle, J. C. (1991). *mu* analysis with real parametric uncertainty. In *[1991] Proceedings of the 30th IEEE conference on decision and control, vol. 2* (pp. 1251–1256).

Zhou, K., & Doyle, J. C. (1998). *Essentials of robust control.* Prentice hall Upper Saddle River, NJ.

Lars A.L. Janssen was born in Nijmegen, the Netherlands, in 1996. He received his M.Sc.-degree (cum laude) in Mechanical Engineering from the Eindhoven University of Technology, Eindhoven, the Netherlands in 2019. Currently, he is a Doctoral Candidate at the Dynamics and Control (DC) group of the Mechanical Engineering Department at Eindhoven University of Technology (TU/e). His current research interest are large-scale interconnected systems, modelling of complex systems and structures, model reduction, and systems engineering.

Bart Besselink is an associate professor at the Bernoulli Institute for Mathematics, Computer Science and Artificial Intelligence of the University of Groningen, the Netherlands. He received the M.Sc. degree (cum laude) in Mechanical Engineering in 2008 and the Ph.D. degree in 2012, both from Eindhoven University of Technology, the Netherlands. He was a short-term visiting researcher at the Tokyo Institute of Technology, Japan, in 2012, and a post-doctoral researcher at the Department of Automatic Control and ACCESS Linnaeus Centre at KTH Royal Institute of Technology, Sweden, between 2012 and 2016. His main research interests are on mathematical systems theory for large-scale interconnected systems, with emphasis on contract-based verification and control, model reduction, and applications in intelligent transportation systems and neuromorphic computing. He is a recipient (with Xiaodong Cheng and Jacquelien Scherpen) of the 2020 Automatica Paper Prize.

Rob H.B. Fey received his M.Sc. degree (cum laude) in Mechanical Engineering and his Ph.D. degree from Eindhoven University of Technology in the Netherlands, in 1987 and 1992, respectively. He was a recipient of the Shell Study Prize for his Ph.D. thesis. From 1992 to 2002, he was a Senior Scientist with the Structural Dynamics Group of the Netherlands Organization for Applied Scientific Research (TNO) in Delft, the Netherlands. Since 2002, he has been with the Dynamics & Control Group, Department of Mechanical Engineering, Eindhoven University of Technology, where he currently is an Associate Professor of Structural Dynamics. He is (co-)author of many refereed journal papers, chapters in books, and conference papers. His general research interests include the modelling, analysis, and validation of the dynamic behaviour of complex structures and (multiphysics) systems. Current focus is on data- and AI-based model updating techniques and model reduction of interconnected systems. His main applications are currently in the fields of High-Tech Systems, Mechatronic Systems and Micro-ElectroMechanical Systems. He is member of the Editorial Board of the Journal of Vibration and Control and the Technical Committee for Vibrations of IFToMM. He was guest editor of the journal Nonlinear Dynamics.

Nathan van de Wouw obtained his M.Sc.-degree (with honours) and Ph.D.-degree in Mechanical Engineering from the Eindhoven University of Technology, the Netherlands, in 1994 and 1999, respectively. He currently holds a full professor position at the Mechanical Engineering Department of the Eindhoven University of Technology, the Netherlands. He has been working at Philips Applied Technologies, The Netherlands, in 2000 and at the Netherlands Organisation for Applied Scientific Research, The Netherlands, in 2001. He has been a visiting professor at the University of California Santa Barbara, U.S.A., in 2006/2007, at the University of Melbourne, Australia, in 2009/2010 and at the University of Minnesota, U.S.A., in 2012 and 2013. He has held a (part-time) full professor position the Delft University of Technology, the Netherlands, from 2015–2019. He has also held an adjunct full professor position at the University of Minnesota, U.S.A, from 2014–2021. He has published the books 'Uniform Output Regulation of Nonlinear Systems: A convergent Dynamics Approach' with A.V. Pavlov and H. Nijmeijer (Birkhauser, 2005) and 'Stability and Convergence of Mechanical Systems with Unilateral Constraints' with R.I. Leine (Springer-Verlag, 2008). In 2015, he received the IEEE Control Systems Technology Award "For the development and application of variable-gain control techniques for high-performance motion systems". He is an IEEE Fellow for his contributions to hybrid, data-based and networked control.